

REVISION #1

The suppression of lone-pair-stereoactivity in $[\text{Cu}^+(\text{As}^{3+}\text{O}_3)_4]$ clusters in dixenite: a tribute to Paul B. Moore

FRANK C. HAWTHORNE^{1,ξ} AND JOHN M. HUGHES²

¹Department of Geological Sciences, University of Manitoba, Winnipeg, Manitoba, R3T 2N2, Canada

²Department of Geology, University of Vermont, Burlington, VT 05405, U.S.A.

ABSTRACT

The crystal structure of dixenite, ideally $\text{Cu}^+\text{Fe}^{3+}\text{Mn}^{2+}_{14}(\text{As}^{5+}\text{O}_4)(\text{As}^{3+}\text{O}_3)_5(\text{SiO}_4)_2(\text{OH})_6$, from Langban, Sweden, was refined to an R_1 -index of 1.58%, and the structure proposed by Araki and Moore (1981) was confirmed and details elucidated. The structure, crystallizing in space group $R3$ with $a = 8.2204(3)$ and $c = 37.485(3)\text{\AA}$, consists of layers of $(\text{Mn}^{2+}, \text{Fe}^{3+})(\text{O},\text{OH})_6$ octahedra linked by $(\text{As}^{5+}\text{O}_4)$ and (SiO_4) tetrahedra, $(\text{As}^{3+}\text{O}_3)$ trigonal pyramids and $(\text{Cu}^+\text{As}^{3+})_4$ tetrahedra. There are five distinct layers in the repeat unit of the cell, four of which are very similar to the layers in mcgovernite. An unusual aspect of one of the trimers of octahedra is that there is a triangular-prismatic hole through the center of the cluster. The $(\text{Cu}^+\text{As}^{3+})_4$ tetrahedra are parts of larger clusters: $[\text{Cu}^+(\text{As}^{3+}\text{O}_3)_4]$ in which four $(\text{As}^{3+}\text{O}_3)$ groups link to a central Cu^+ which occupies the positions normally taken by the stereoactive lone-pairs of electrons that generally characterize As^{3+} in triangular-pyramidal coordination by O. Thus the stereoactive lone-pair behavior that is characteristic of $(\text{As}^{3+}\text{O}_3)$ trigonal pyramids is suppressed by the coordination of Cu^+ by four As^{3+} ions.

Keywords: Dixenite, crystal structure, lone-pair electrons, Paul B. Moore

^ξ E-mail: Frank.Hawthorne@umanitoba.ca

27

INTRODUCTION

28

29

30

31

32

33

34

35

36

37

38

39

40

Paul Brian Moore (1940-2019) was one of the giants of Mineralogy, and his legacy lives in the numerous papers he published in his distinguished career. His contributions to Mineralogy were celebrated in a recent memorial (Hawthorne et al. 2019) that stated that he was the greatest mineralogist of the 20th century. Professor Moore and his colleagues solved numerous complex structures in an age before (usually) routine solution of crystal structures using Direct Methods was possible, stretching the limits of equipment and computational resources of that time. As noted in his Memorial, even in retirement Paul never stopped thinking about problems involving crystal structures. In addition to being involved with new atomic arrangements, he urged colleagues to re-examine some of his earlier solutions that were done with the diffraction equipment of an earlier day. One of those structures was that of dixenite, which was a frequent source of conversations with his colleagues. At the time of his death, Professor Moore was urging both of us to re-examine the dixenite structure, and we are pleased to offer the results of that work here.

41

42

43

44

45

46

47

48

49

Dixenite, ideally $\text{Cu}^+\text{Fe}^{3+}\text{Mn}^{2+}_{14}(\text{As}^{5+}\text{O}_4)(\text{As}^{3+}\text{O}_3)_5(\text{SiO}_4)_2(\text{OH})_6$, is of considerable interest because it has a novel metallic cluster, ideally $(\text{Cu}^+\text{As}^{3+}_4)$, embedded in an oxide environment (Araki and Moore 1981), an atomic arrangement that had not been observed previously in any structure. At the same time, Moore and Araki (1979) found another metallic cluster, $(\text{Mn}^+\text{As}^{3+}_6)$, embedded in an oxide environment in magnussonite, ideally $\text{Mn}^{2+}_{18}[\text{Mn}^+\text{As}^{3+}_6\text{O}_{18}]_2\text{Cl}_2$. As far as we are aware, these are the only examples of such clusters found in minerals, and Paul B. Moore (personal communication) was keen to see confirmation of these findings by more accurate modern instrumentation. Moreover, both these minerals occur only in the (Fe-Mn)-oxide ore deposits at Långban, Sweden (Moore 1970; Holtstam and Langhof

50 1999; Lundström 1999; Bollmark 1999; Nysten et al. 1999), and we have a long-term interest in
51 the basic Mn-arsenate-silicate minerals from this locality (Hawthorne 2018; Hawthorne et al.
52 2013; Cooper and Hawthorne 1999, 2012).

53

54 **SAMPLE PROVENANCE**

55 Both samples examined here are from Långban. One sample was obtained from the U.S.
56 National Museum of Natural History (C4440, provided to Paul B. Moore) and the other from the
57 late Mark Feingloss, a well-known mineral collector from Duke University. The structural results
58 are virtually identical and we present only one refinement here.

59

60 **CRYSTAL STRUCTURE**

61 **Data collection and refinement**

62 A crystal fragment from NMNH C4440 was mounted on a Bruker Apex CCD
63 diffractometer equipped with graphite-monochromated Mo $K\alpha$ radiation. Refined cell
64 parameters and other crystal data are listed in the deposited CIF file. Redundant data were
65 collected for a sphere of reciprocal space, and were integrated and corrected for Lorentz and
66 polarization factors and absorption using the Bruker program SAINTPLUS.

67 The atomic arrangement was solved independently of that given by Araki and Moore
68 (1981), and hydrogen positions were located using difference-Fourier maps. The structure is in
69 close agreement with that of Araki and Moore (1981); we have retained their original atom
70 nomenclature in this paper. Refinement was done with anisotropic-displacement parameters for
71 all atoms except H. Table 1 lists the refined atom parameters, Table 2 lists selected interatomic
72 distances, and Table 3 gives the bond-valence table (vu; valence units) calculated with the

73 parameters of Gagné and Hawthorne (2015). A CIF has been deposited which contains further
74 details of crystal data and structure refinement¹.

75 **Site populations**

76 The atomic arrangement is virtually identical with that given by Araki and Moore (1981),
77 although of much greater precision. There are three As sites with associated coordinations, bond
78 lengths and angles characteristic of As³⁺. Each As³⁺ is coordinated by three O²⁻ ions at distances
79 from 1.726-1.776 Å, in the range of ^[3]As³⁺-O distances shown by inorganic crystal-structures:
80 1.671-1.845 Å (Gagné and Hawthorne 2018) and close to the grand mean ^[3]As³⁺-O distance of
81 1.776 Å. There are three T sites that have site-scattering values between Si and As; each site is
82 coordinated by a tetrahedral arrangement of O atoms, and have T-O distances (Table 2) that are
83 intermediate between those expected for ^[4]Si-O and ^[4]As⁵⁺-O in oxide and oxysalt structures
84 (Gagné and Hawthorne 2018). There are six M sites that have site-scattering values characteristic
85 of Mn and Fe and that are octahedrally coordinated by O atoms. The observed interatomic
86 distances (Table 2) indicate that six of these sites are occupied by Mn²⁺ with minor Fe²⁺. The site
87 scattering at the M3 site indicates that this site is occupied by a transition metal. The <M3-O>
88 bond length is 2.057 Å, significantly longer than the grand <Fe³⁺-O> distance of 2.015 Å
89 reported by Gagné and Hawthorne (2020) for oxide and oxysalt structures. Thus, in addition to
90 Fe³⁺, M3 must be occupied partly by Fe²⁺ and/or Mn²⁺, in accord with the incident bond-valence
91 sum at M3 of 2.67 vu (Table 3). Polyhedra are labelled by the identity of the ion/atom at the
92 central site: thus the coordination octahedron of Mn²⁺ at the M1 site, Mn²⁺O₆, is denoted as the

¹ Deposit item AM-20-xx1 for CIF file. Deposit items are available two ways: for paper copies, contact the Business Office of the Mineralogical Society of America (see inside front cover of recent issue) for price information. For an electronic copy, visit the MSA web site at <http://www.minsocam.org>, go to the *American Mineralogist* Contents, find the table of contents for the specific volume/issue wanted, and then click on the deposit link there.

93 M1 octahedron. The bond valences incident at the O anions (Table 3) show that OH1 and OH2
94 are hydroxyl groups and the remaining anions are O^{2-} . The site-scattering values and mean bond
95 lengths are in accord with the formula $Cu^+Fe^{3+}Mn^{2+}_{14}(As^{5+}O_4)(As^{3+}O_3)_5(SiO_4)_2(OH)_6$ assigned
96 by Araki and Moore (1981).

97 **Bond topology**

98 The dixenite structure contains fifteen layers of approximately close-packed polyhedra
99 that comprise one translation along **c**. In space group *R3* five symmetrically and bond-
100 topologically distinct layers are stacked orthogonal to the **c**-axis to give the ~ 37.5 Å repeat in the
101 **c** direction. The five distinct layers of cation-centered polyhedra are labelled $m = 0-4$ in Figure 1,
102 and these layers are shown in plan in Figure 2 where they are compared with similar layers in the
103 crystal structure of mcgovernite (Hawthorne 2018).

104 At $m = 0$ (Fig. 2a), the layer consists of M5 octahedra containing Mn^{2+} and two distinct
105 tetrahedra, T2As and T3As, that contain As^{5+} and Si with As^{5+} dominant at both T sites (Table
106 2). The M5 octahedron shows a large dispersion of bond lengths: 2.086-2.735 Å (Table 2) and
107 the question arises as to the coordination number of Mn^{2+} at the M5 site. Gagné and Hawthorne
108 (2020) list the range of observed $[^6]Mn^{2+}-O$ distances in oxide and oxysalt structures as 1.968-
109 2.798 Å and the range of $\langle [^6]Mn^{2+}-O \rangle$ distances as 2.134-2.305 Å; the observed M5-O distances
110 fall within these ranges (Table 2) and hence we consider the M5 polyhedron as an octahedron.
111 The M5 octahedra share edges to form a very unusual trimer (Fig. 3a). Edge-sharing between
112 octahedra is extremely common in oxide and oxysalt structures, and the usual arrangement of a
113 trimer of edge-sharing octahedra is shown in Fig. 3b for the M6 octahedra in layer $m = 4$, in
114 which the shared edges (shown in red in Fig. 3) meet at the centre of the trimer. In the M5 trimer
115 (Fig. 3a), the shared edges form the vertical (sub-parallel to **c**) edges of a twisted triangular prism

116 that forms an empty channel through the center of the M5 trimer. The reason for this
117 arrangement is not apparent, but may be related to the different stoichiometries of the two
118 arrangements: M5: $[M_3O_{12}]$; M6: $[M_3O_{13}]$. The M5 trimers link into a sheet by sharing corners
119 with tetrahedra; the T2As tetrahedron points in the +c direction and the T3As tetrahedron points
120 in the -c direction (Fig. 2a). Fig. 2b shows the analogous layer in the structure of mcgovernite in
121 which the unit cell is shifted relative to that in dixenite by $1/3 \ 2/3$ in the (001) plane. In
122 mcgovernite, there is only one crystallographically distinct tetrahedron in this layer and this
123 tetrahedron is occupied by Si. The Z1 tetrahedron in mcgovernite occupies a position similar to
124 the M5 octahedron in dixenite but does not link to other Z1 tetrahedra by sharing vertices;
125 however, the pattern of Z1 tetrahedra in the $m = 7$ layer in mcgovernite (Fig. 2b) resembles the
126 pattern of M5 polyhedra in the $m = 0$ layer of dixenite (Fig. 2a).

127 At $m = 1$ (Fig. 2c), the layer consists of trimers of edge-sharing M4 octahedra linked by
128 sharing corners with $As^{3+}O_3$ groups. In the topologically analogous layer in mcgovernite ($m = 6$;
129 Fig. 2d), the trimers of M5 octahedra are linked by SiO_4 groups. In dixenite, the corners of the
130 unit cell are situated at holes in the layer (Fig. 2c). This hole has a very low occupancy by Cu
131 (M2A site; Table 2) and we have denoted the corresponding layer as $m = 1'$ as it is disordered
132 with the $m = 1$ layer. In the $m = 1'$ layer (Fig. 2e) in dixenite, there is an M2A octahedron at the
133 origin of the unit cell that shares edges with the octahedra of the M4 trimers to form an
134 interrupted sheet of octahedra with $As^{3+}O_3$ groups occupying the interstices. A similar layer
135 occurs in mcgovernite (Fig. 2f) except that the $As^{3+}O_3$ groups in dixenite are replaced with SiO_4
136 groups in mcgovernite.

137 The $m = 2$ layer in dixenite (Fig. 2g) consists of isolated $\text{Cu}^+\text{As}^{3+}_4$ groups that link to
138 isolated M1 and M2 octahedra through two distinct As^{3+}O_3 groups: As2 and As3. There is no
139 analogous layer in the structure of mcgovernite.

140 In the $m = 3$ layer in dixenite (Fig. 2h), trimers of M7 octahedra share edges with a single
141 M3 octahedron to form an interrupted sheet in which As^{3+}O_3 groups link to the surrounding M7
142 octahedra. The analogous $m = 3$ layer in mcgovernite (Fig. 2i) has the same connectivity except
143 that there are As^{5+}O_4 tetrahedra in the interstices of the sheet and the M1 octahedron, although
144 dominated by Mn^{2+} , is occupied by a considerable amount of Mg.

145 The $m = 4$ layer in dixenite (Fig. 2j) consists of edge-sharing trimers of M6 octahedra
146 linked by sharing corners with SiO_4 tetrahedra; note that this layer differs from the $m = 1$ layer in
147 dixenite in that the trimers have different orientations (Figs. 2c, 2j). The analogous layer in
148 mcgovernite is $m = 2A$ (Fig. 2k) in which the trimers are linked by As^{3+}O_3 groups.

149 **The ($\text{Cu}^+\text{As}^{3+}_4$) arrangement**

150 There are two Cu sites, Cu1 and Cu2, that are 0.879(8) Å apart, and hence both cannot be
151 locally occupied. The two sites are jointly coordinated by a trigonal bipyramid of As^{3+} ions (Fig.
152 4). The refined site-scattering at the two Cu sites, in accord with aggregate occupancy of the two
153 Cu sites, is $\text{Cu}^{+}_{0.85} + \square_{0.15}$, and at any one Cu1-Cu2 pair, one Cu site is occupied by Cu^+ and the
154 locally associated Cu site is vacant. The neighboring As sites are fully occupied by As^{3+} . Where
155 both sites are locally not occupied, the lone pairs on the locally associated As^{3+} ions will point
156 toward the unoccupied Cu1 and Cu2 sites.

157 The coordination of each of the Cu sites is illustrated in Figure 4 in which each Cu^+ ion is
158 [4]-coordinated by As^{3+} . Each coordinating As^{3+} ion bonds to three O atoms at distances of ~ 1.76
159 Å and one Cu^+ ion at distances of 2.34-2.50 Å. The oxygen atoms bonded to As^{3+} are arranged in

160 a trigonal prismatic arrangement; the range of As^{3+} -O distances (1.73-1.78 Å) are well within the
161 range of 1.67-1.85 Å given by Gagné and Hawthorne (2018) for $^{[31]}\text{As}^{3+}$ -O distances in all
162 inorganic oxide and oxysalt compounds, and the mean distance of 1.76 Å is close to their grand
163 mean $^{[31]}\text{As}^{3+}$ -O distance of 1.776 Å. Thus the Cu^+ ions are each coordinated by four As^{3+} - O_3
164 groups in a tetrahedral arrangement. Such As^{3+} - O_3 groups are characterized by a stereoactive
165 lone-pair of electrons extending away from the As^{3+} ion on the side opposing the three O atoms.
166 In the atom arrangements shown in Figure 4, it is apparent that the stereoactive character of the
167 lone electron pair is suppressed by the presence of Cu^+ as a fourth ligand to As^{3+} : $\text{As}^{3+}\text{O}_3\text{Cu}^+$.
168 The Cu1-As distances are 2.400×3 , 2.342 and 3.378 Å and the Cu2-As distances are 2.369×3 ,
169 2.499 and 3.221 Å. It is apparent that Cu1 and Cu2 are each coordinated by four As^{3+} ions and
170 the longer distances > 3.2 Å are not bonded interactions. Inspection of Figure 4 shows that the
171 splitting of Cu into two separate sites, Cu1 and Cu2, is driven by the need for Cu^+ to shorten the
172 bond to As^{3+} , either As1 or As2, and the 1:1 split suggests that this is not long-range ordered.

173 Cu^+ - As^{3+} interactions are not common in crystal structures, but such bonds have been
174 reported in a few metallo-organic structures. Karagiannidis et al. (1991a) lists a single Cu^+ - As^{3+}
175 bond of 2.371(1) Å in $[\text{Cu}(\text{tclH})_2(\text{AsPh}_3)\text{Br}]$ in a $(\text{Cu}^+\text{As}^{3+}\text{S}^{2-}_2\text{Br}^-)$ tetrahedron, and Karagiannidis
176 et al. (1991b) lists Cu^+ - As^{3+} distances of 2.411 (2) and 2.372(2) Å in $\text{Cu}(\text{tclH})(\text{AsPh}_3)_2\text{Br}$ in a
177 $(\text{Cu}^+\text{As}^{3+}_2\text{S}^{2-}_2\text{Br}^-)$ tetrahedron. The distances are sufficiently similar to those reported for Cu^+ -
178 As^{3+} in Table 2 to suggest that the atomic arrangements shown in Fig. 4 are chemically
179 reasonable.

180 **Fitting the $[\text{Cu}^+(\text{As}^{3+}\text{O}_3)_4]$ clusters into the layered structure**

181 The $[\text{Cu}^+(\text{As}^{3+}\text{O}_3)_4]$ clusters are quite complicated atom arrangements and it is surprising
182 to encounter them in a close-packed structure. The way in which they are incorporated is

183 illustrated in Fig. 5. There is a layer of trimers of Mn^{2+} octahedra (Fig. 5a) in which adjacent
184 trimers provide a triangle of O atoms that link to As^{3+} at the apical position of the $(\text{Cu}^+\text{As}^{3+}_4)$
185 tetrahedron centered at the Cu2 site. Figure 5b shows a view of the same arrangement in the
186 other direction where the linkage of the other $(\text{As}^{3+}\text{O}_3)$ groups to the underside of the M4 trimers
187 and to the underlying layer of M(7) trimers is apparent. Thus the two layers of M-trimers are
188 linked by the $[\text{Cu}^+(\text{As}^{3+}\text{O}_3)_4]$ cluster involving the Cu^+ ion at the Cu2 site. As is apparent from
189 Figure 4, the corresponding $[\text{Cu}^+(\text{As}^{3+}\text{O}_3)_4]$ cluster involving the Cu1 site points in the opposite
190 direction.

191 Figure 6 compares the M(4)-As(1) layer in dixenite with the M(2)-As(3) layer in
192 mcgovernite. Both layers consist of trimers of octahedra linked by $(\text{As}^{3+}\text{O}_3)$ groups but the
193 patterns of distribution of the $(\text{As}^{3+}\text{O}_3)$ groups are complementary. The layer in mcgovernite
194 (Fig. 6b) is disordered with the layer shown in Figure 6c; in that layer the As^{3+}O_3 groups are
195 replaced by a trimer of Z(2) octahedra in which the octahedra are only partly occupied. It is
196 striking that the other layers in mcgovernite with the same pattern of trimers and linking (SiO_4)
197 groups (layers $m = 4$ and $m = 6$; Hawthorne 2018) do not show this disorder. It is not clear at the
198 moment what is causing the presence of the unusual $[\text{Cu}^+(\text{As}^{3+}\text{O}_3)_4]$ cluster in dixenite and the
199 analogous disordered layers of trimers of partly occupied octahedra in mcgovernite. It is to be
200 hoped that a more comprehensive examination of all the basic manganese-silicate-arsenate-
201 arsenite minerals (including two potentially new minerals, work in progress) will allow us to
202 understand why $\text{Cu}^+\text{-As}^{3+}$ bonds form in some of these structures.

203

IMPLICATIONS

204 The basic manganese-iron arsenate-arsenite-silicate minerals of the Långban-type
205 deposits in Bergslagen, Sweden, form a family of very complicated layered structures, several of

206 which contain local exotic atomic arrangements embedded within their close-packed structures.
207 Examples are the $[\text{Cu}^+(\text{As}^{3+}\text{O}_3)_4]$ cluster and the $[\text{Mn}^{2+}_3\text{O}_{12}]$ cluster reported here in dixenite and
208 the local replacement of an As^{3+}O_3 group by a $[\text{Mg},\text{Mn}^{2+}_3\text{O}_{13}]$ cluster in mcgovernite and
209 carlfrancisite (Hawthorne 2018). In the same type of deposit, magnussonite (Moore and Araki
210 1979), although a defect-fluorite structure, contains a $[\text{Mn}^+\text{As}^{3+}_6]$ cluster. The presence of these
211 exotic clusters in densely packed Mn^{2+} octahedra is not understood at the moment, but may be
212 related to the relaxation of accumulated strain. There is the potential to incorporate exotic
213 clusters with unusual properties into dense oxide matrices, and hence develop materials with
214 desirable physical properties if the details of their incorporation can be understood. With only
215 two minerals that contain metallic clusters in an oxide matrix, little is known about such clusters
216 and compounds. In both minerals, the semimetal As is an essential component of the cluster, and
217 that class of elements may facilitate their formation in oxide matrices. Metal clusters on two-
218 dimensional substrates are studied extensively in the science of non-volatile memory materials,
219 and the existence of such clusters in three-dimensional mineral structures may provide a template
220 for important industrial materials. The detailed re-examination of dixenite described herein, and
221 the discovery and description of increasingly complex mineral structures over the past decade,
222 illustrate that minerals provide a rich template for important synthetic materials.

223 **ACKNOWLEDGMENTS**

224 This work was supported by a Discovery grant from the Natural Sciences and
225 Engineering Research Council of Canada and a Canada Foundation for Innovation Grant, both to
226 FCH, and by NSF grants EAR-0003201 and MRI 1039436 to JMH. Both authors are also
227 grateful for years of interaction with the late Paul Brian Moore and for his suggestion that we
228 look at dixenite more closely. The authors are grateful for the editorial handling of Oliver

229 Tschauner and the detailed reviews of Anthony R. Kampf, Martin Kunz, and the *American*
230 *Mineralogist* Technical Editor.

231

232

233

234

235

236

237

238

239

240

241

242

243

244

245

246

247

248
249
250
251
252
253
254
255
256
257
258
259
260
261
262
263
264
265
266
267
268
269
270
271

REFERENCES CITED

- Araki, T., and Moore, P.B. (1981) Dixenite, $\text{Cu}^{1+}\text{Mn}_{14}^{2+}\text{Fe}^{3+}(\text{OH})_6(\text{As}^{3+}\text{O}_3)_5(\text{As}^{5+}\text{O}_4)$: metallic $[\text{As}_4^{3+}\text{Cu}^{1+}]$ clusters in an oxide matrix. *American Mineralogist*, 66, 1263-1273.
- Bollmark, B. (1999) Some aspects of the origin of the deposit. *In* Långban: the Mines, their Minerals, Geology and Explorers (D. Holtstam & J. Langhof, eds.). Raster Förlag, Stockholm, Sweden (43-49).
- Cooper, M.A. and Hawthorne, F.C. (1999) The effect of differences in coordination on ordering of polyvalent cations in close-packed structures: the crystal structure of arakiite and comparison with hematolite. *The Canadian Mineralogist*, 37, 1471–1482.
- Cooper, M.A. and Hawthorne, F.C. (2012) The crystal structure of kraisslite, $^{[4]}\text{Zn}_3(\text{Mn},\text{Mg})_{25}(\text{Fe}^{3+},\text{Al})(\text{As}^{3+}\text{O}_3)_2[(\text{Si},\text{As}^{5+})\text{O}_4]_{10}(\text{OH})_{16}$, from the Sterling Hill mine, Ogdensburg, Sussex County, New Jersey, USA. *Mineralogical Magazine*, 76, 2819–2836.
- Gagné, O. & Hawthorne, F.C. (2015) Comprehensive derivation of bond-valence parameters for ion pairs involving oxygen. *Acta Crystallographica*, B71, 562–578.
- Gagné, O. C. and Hawthorne, F.C. (2018) Bond-length distributions for ions bonded to oxygen: Metalloids and post-transition metals. *Acta Crystallographica*, B74, 63-78.
- Gagné, O.C. & Hawthorne, F.C. (2020) Bond-length distributions for ions bonded to oxygen: Results for the transition metals and quantification of the factors underlying polyhedral distortion via bond-length variation. *IUCrJ*, 7, 581-629.
- Hawthorne, F.C. (2018): Long-range and short-range cation order in the crystal structures of carlfrancisite and mcgovernite. *Mineralogical Magazine*, 82, 1101-1118.
- Hawthorne, F.C., Abdu, Y.A., Ball, N.A. and Pinch, W.W. (2013) Carlfrancisite: $\text{Mn}^{2+}_3(\text{Mn}^{2+},\text{Mg},\text{Fe}^{3+},\text{Al})_{42}[\text{As}^{3+}\text{O}_3]_2(\text{As}^{5+}\text{O}_4)_4[(\text{Si},\text{As}^{5+})\text{O}_4]_6[(\text{As}^{5+},\text{Si})\text{O}_4]_2(\text{OH})_{42}$, a new

- 272 arseno-silicate mineral from the Kombat mine, Otavi valley, Namibia. American
273 Mineralogist, 98, 1693–1696.
- 274 Hawthorne, F.C., Kampf, A.R., and Hervig, R. (2019) Memorial of Paul Brian Moore, 1940-
275 2019. American Mineralogist, 104, 1062-1063.
- 276 Holtstam, D. and Langhof, J. (editors) (1999) Långban, the Mines, their Minerals, History and
277 Explorers. Raster Förlag, Stockholm, pp. 215.
- 278 Karagiannidis, P., Akrivos, P.D., Mentzafos, D. and Terzis, A. (1991a) New class of Cu(I)
279 complexes with 2-thioxohexamethyleneimine (tclH) and Group V_A donors. Crystal
280 structure of [Cu(tclH)₂(AsPh₃)Br]. Inorganica Chimica Acta, 181, 263-267.
- 281 Karagiannidis, P., Akrivos, P., Aubry, A., and Skoulika, S. (1991b) Synthesis and study of
282 mixed ligand monomer Cu(I) compounds with Cu-As bonds. Crystal and molecular
283 structure of bis(triphenylarsine)-(2-thioxohexamethyleneimine)copper(I) bromide.
284 Inorganica Chimica Acta, 188, 79-83.
- 285 Lundström, I. (1999) General geology of the Bergslagen ore region. *In* Långban: the Mines, their
286 Minerals, Geology and Explorers (D. Holtstam & J. Langhof, eds.). Raster Förlag,
287 Stockholm, Sweden (19-27).
- 288 Moore, P.B. (1970) Mineralogy and chemistry of Långban type deposits in Bergslagen, Sweden.
289 Mineralogical Record **1**, 154-172.
- 290 Moore, P. B. and Araki, T. (1979) Magnussonite, manganese arsenite, a fluorite derivative
291 structure. American Mineralogist, 64, 390-401.
- 292 Nysten, P., Holtstam, D. & Jonsson, E. (1999) The Långban minerals. *In* Långban: the Mines,
293 their Minerals, Geology and Explorers (D. Holtstam & J. Langhof, eds.). Raster Förlag,
294 Stockholm, Sweden (89-183).
- 295

296 **Table 1.** Atom coordinates and equivalent isotropic atom-displacement parameters (\AA^2)
 297 for dixenite. $U(\text{eq})$ is defined as one third of the trace of the orthogonalized U_{ij} tensor.

298

| Atom | x/a | y/b | z/c | U(eq) | Occ. |
|------|------------|-------------|-------------|-------------|--|
| As1 | 1/3 | 2/3 | 0.93013(3) | 0.00961(13) | As _{1.00} |
| As2 | 2/3 | 1/3 | 0.74936(3) | 0.00925(13) | As _{1.00} |
| As3 | 0.91124(5) | 0.62586(6) | 0.68425(3) | 0.01006(9) | As _{1.00} |
| T1SI | 1/3 | 2/3 | 0.81217(5) | 0.0065(5) | Si _{0.946(7)} As _{0.054} |
| T2AS | 0 | 0 | 0.85378(4) | 0.0079(3) | Si _{0.458} As _{0.542(7)} |
| T3AS | 2/3 | 1/3 | 0.88640(3) | 0.0073(3) | Si _{0.275} As _{0.725(7)} |
| M1 | 0 | 0 | 0 | 0.01162(19) | Mn _{1.00} |
| M2 | 2/3 | 1/3 | 0.99435(5) | 0.0177(4) | Mn _{0.937(5)} |
| M2A | 2/3 | 1/3 | 0.9635(7) | 0.030(6) | Cu _{0.063} |
| M3 | 0 | 0 | 0.74267(4) | 0.0091(3) | Fe _{0.943(6)} |
| M4 | 0.95815(9) | 0.73646(9) | 0.93256(3) | 0.01243(13) | Mn _{1.00} |
| M5 | 0.58214(9) | 0.66184(10) | 0.87042(3) | 0.01397(13) | Mn _{1.00} |
| M6 | 0.89166(9) | 0.60100(9) | 0.80761(3) | 0.01194(13) | Mn _{1.00} |
| M7 | 0.57710(9) | 0.68485(9) | 0.73874(3) | 0.01028(12) | Mn _{1.00} |
| Cu1 | 2/3 | 1/3 | 0.68694(5) | 0.0104(5) | Cu _{0.663(7)} |
| Cu2 | 1/3 | 2/3 | 0.99682(19) | 0.0162(19) | Cu _{0.190(6)} |
| O1 | 0 | 0 | 0.89791(15) | 0.0155(10) | O _{1.00} |
| O2 | 1/3 | 2/3 | 0.17418(14) | 0.0153(10) | O _{1.00} |
| O3 | 1/3 | 2/3 | 0.76863(13) | 0.0091(8) | O _{1.00} |
| O4 | 0.9104(5) | 0.5555(4) | 0.97864(9) | 0.0162(6) | O _{1.00} |
| O5 | 0.5305(4) | 0.8340(4) | 0.90522(8) | 0.0115(5) | O _{1.00} |
| O6 | 0.7168(4) | 0.5446(4) | 0.90093(9) | 0.0130(6) | O _{1.00} |
| O7 | 0.8341(4) | 0.7922(4) | 0.83826(9) | 0.0105(5) | O _{1.00} |
| O8 | 0.4810(4) | 0.8724(4) | 0.82948(8) | 0.0125(5) | O _{1.00} |
| O9 | 0.6318(4) | 0.4991(4) | 0.77256(8) | 0.0105(5) | O _{1.00} |
| O10 | 0.8531(4) | 0.7722(4) | 0.70923(9) | 0.0129(5) | O _{1.00} |
| O11 | 0.5380(4) | 0.8815(4) | 0.70443(8) | 0.0108(5) | O _{1.00} |
| OH1 | 0.7869(4) | 0.8217(4) | 0.96239(9) | 0.0125(5) | O _{1.00} |
| H1 | 0.697(8) | 0.719(8) | 0.9679(15) | 0.008(12) | H _{1.00} |
| OH2 | 0.7648(4) | 0.9183(4) | 0.77301(9) | 0.0116(5) | O _{1.00} |
| H2 | 0.758(11) | 0.852(11) | 0.793(2) | 0.04(2) | H _{1.00} |

300

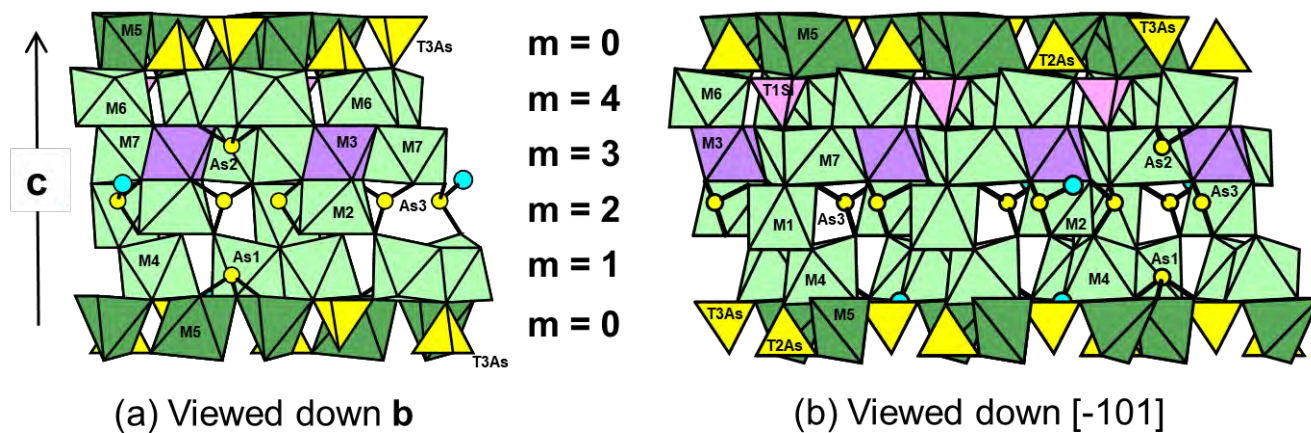
301 **Table 2.** Selected bond distances (Å) in dixenite. Bond distances in italics are to second
 302 cation occupant in split site and are not included in mean

| | | | |
|-----|-----------------------|------------------------|-----------------------|
| 304 | As1 - Distance | As2 - Distance | As3 - Distance |
| 305 | O5(×3) 1.7782(31) | O9(×3) 1.7567(29) | O4 1.7300(32) |
| 306 | Mean 1.778 | Mean 1.757 | O11 1.7634(28) |
| 307 | | | O10 1.7684(30) |
| 308 | | | Mean 1.754 |
| 309 | | | |
| 310 | T1SI - Distance | T2AS - Distance | T3AS - Distance |
| 311 | O3 1.6320(53) | O1 1.6544(56) | O6(×3) 1.6634(30) |
| 312 | O8(×3) 1.6438(32) | O7(×3) 1.6694(28) | O2 1.7076(54) |
| 313 | Mean 1.641 | Mean 1.666 | Mean 1.674 |
| 314 | | | |
| 315 | M1 - Distance | M2 - Distance | M2A - Distance |
| 316 | OH1(×3) 2.1533(33) | <i>M2A</i> 1.1580(250) | <i>M2</i> 1.1580(250) |
| 317 | O11(×3) 2.2318(30) | O4(×3) 2.0094(32) | O4(×3) 2.0036(78) |
| 318 | Mean 2.193 | O10(×3) 2.4437(35) | Mean 2.004 |
| 319 | | Mean 2.227 | |
| 320 | | | |
| 321 | M3 - Distance | M4 - Distance | M5 - Distance |
| 322 | OH2(×3) 2.0455(31) | O5 2.1537(30) | O8 2.0859(30) |
| 323 | O10(×3) 2.0675(31) | OH1 2.1584(32) | O5 2.1177(30) |
| 324 | Mean 2.057 | O6 2.1679(31) | O6 2.1282(31) |
| 325 | | OH1 2.1701(31) | O7 2.1614(31) |
| 326 | | O4 2.1832(32) | O5 2.4136(32) |
| 327 | | O1 2.3985(30) | O8 2.7354(32) |
| 328 | | Mean 2.205 | Mean 2.274 |
| 329 | | | |
| 330 | M6 - Distance | M7 - Distance | Cu1 - Distance |
| 331 | O8 2.0777(31) | OH2 2.1803(30) | <i>Cu2</i> 0.8789(67) |
| 332 | O7 2.1815(30) | O9 2.1973(29) | As3(×3) 2.2361(4) |
| 333 | OH2 2.2454(32) | O11 2.2112(29) | As2 2.3400(18) |
| 334 | O9 2.2460(30) | O3 2.2347(25) | Mean 2.262 |
| 335 | O9' 2.2805(30) | O11 2.2762(30) | |
| 336 | O2 2.3968(29) | O10 2.2928(31) | |
| 337 | Mean 2.238 | Mean 2.232 | |
| 338 | | | |
| 339 | Cu2 - Distance | | |
| 340 | <i>Cu1</i> 0.8789(67) | | |
| 341 | As3(×3) 2.3654(24) | | |
| 342 | As1 2.5001(72) | | |
| 343 | Mean 2.399 | | |

| Table 3. Bond-valence (<i>vu</i>) table for dixenite | | | | | | | | | | | | | | |
|--|---------------------|---------------------|---------------------|---------------------|--------------|---------------------|---------------------|---------------------|---------------------|---------------------|---------------------|---------------------|---------------|------|
| | <i>M</i> (1) | <i>M</i> (2) | <i>M</i> (3) | <i>M</i> (4) | <i>M</i> (5) | <i>M</i> (6) | <i>M</i> (7) | <i>T</i> (1) | <i>T</i> (2) | <i>T</i> (3) | <i>As</i> (1) | <i>As</i> (2) | <i>As</i> (3) | Σ |
| O(1) | | | | 0.21 ^{x3→} | | | | | 1.17 | | | | | 1.80 |
| O(2) | | | | | | 0.21 ^{x3→} | | | | 1.08 | | | | 1.71 |
| O(3) | | | | | | | 0.31 ^{x3→} | 1.01 | | | | | | 1.94 |
| O(4) | | 0.52 ^{x3↓} | | 0.34 | | | | | | | | | 1.11 | 1.97 |
| O(5) | | | | 0.37 | 0.40 0.20 | | | | | | 0.99 ^{x3↓} | | | 1.96 |
| O(6) | | | | 0.36 | 0.39 | | | | | 1.22 ^{x3↓} | | | | 1.97 |
| O(7) | | | | | 0.36 | 0.35 | | | 1.12 ^{x3↓} | | | | | 1.83 |
| O(8) | | | | | 0.44 0.09 | 0.45 | | 0.98 ^{x3↓} | | | | | | 1.96 |
| O(9) | | | | | | 0.30 0.27 | 0.33 | | | | | 1.04 ^{x3↓} | | 1.94 |
| O(10) | | 0.18 ^{x3↓} | 0.43 ^{x3↓} | | | | 0.27 | | | | | | 1.01 | 1.89 |
| O(11) | 0.31 ^{x3↓} | | | | | | 0.32 0.28 | | | | | | 1.03 | 1.94 |
| OH(1) | 0.37 ^{x3↓} | | | 0.37 0.36 | | | | | | | | | | 1.10 |
| OH(2) | | | 0.46 ^{x3↓} | | | 0.30 | 0.35 | | | | | | | 1.11 |
| Σ | 2.04 | 2.10 | 2.67 | 2.01 | 1.88 | 1.88 | 1.86 | 3.95 | 4.53 | 4.74 | 2.97 | 3.12 | 3.15 | |
| | 2 | 3 | 3 | 2 | 2 | 2 | 2 | 4.05 | 4.54 | 4.72 | 3 | 3 | 3 | |

345

346



347

348

349

FIGURE 1. The five unique layers in dixenite ($m = 0-4$) that stack along the c-axis.

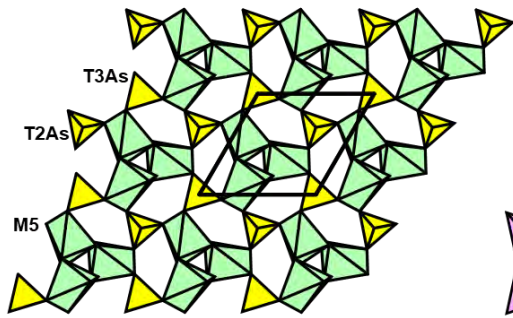
350

351

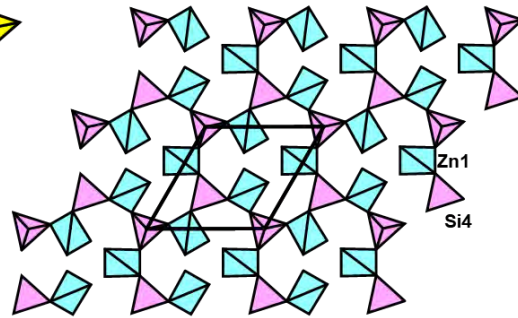
352

353

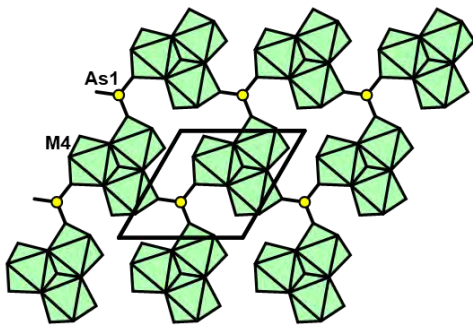
354



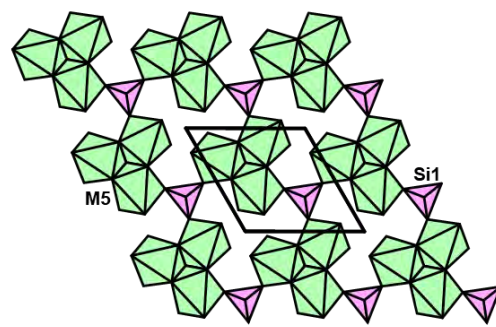
(a) Dixenite: $m = 0$



(b) McGovernite: $m = 7$

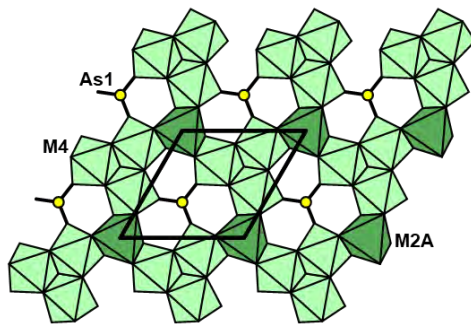


(c) Dixenite: $m = 1$

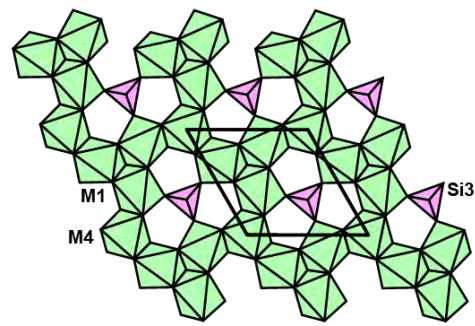


(d) McGovernite: $m = 6$

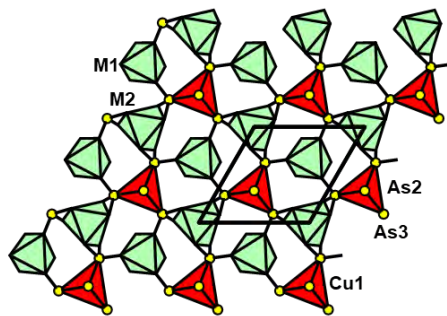
355



(e) Dixenite: $m = 1'$



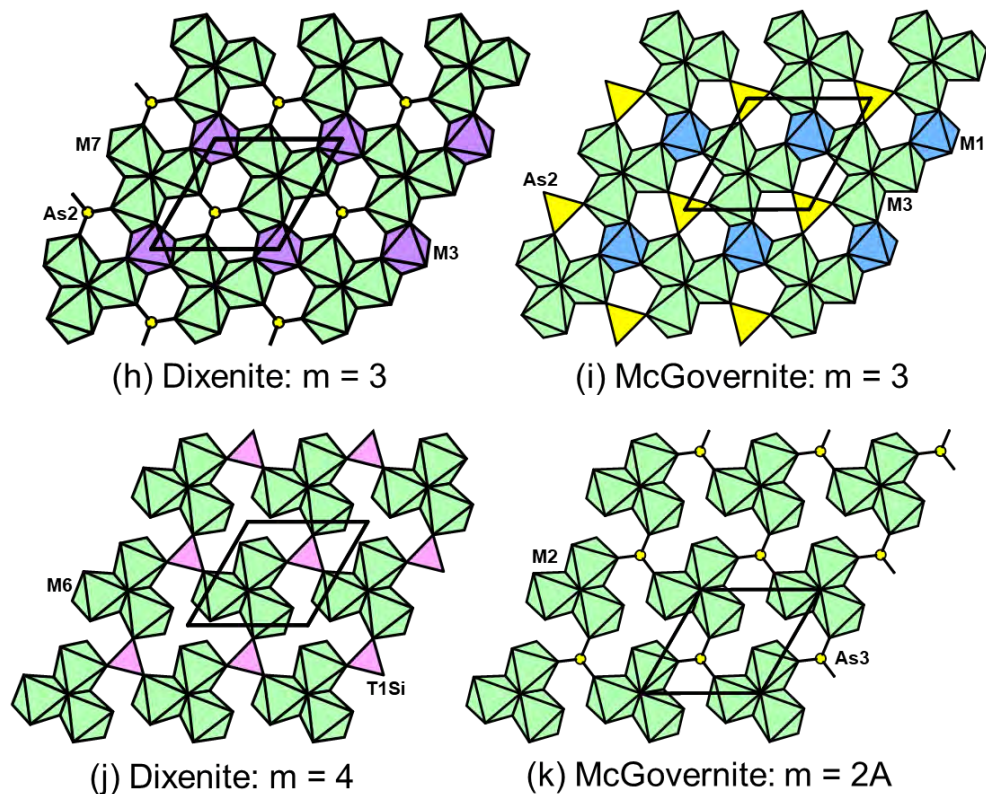
(f) McGovernite: $m = 5$



(g) Dixenite: $m = 2$

356

357



358

359

360 **FIGURE 2.** Plan views of layers in dixenite compared to similar layers in mcgovernite. Detailed
361 comparisons given in text.

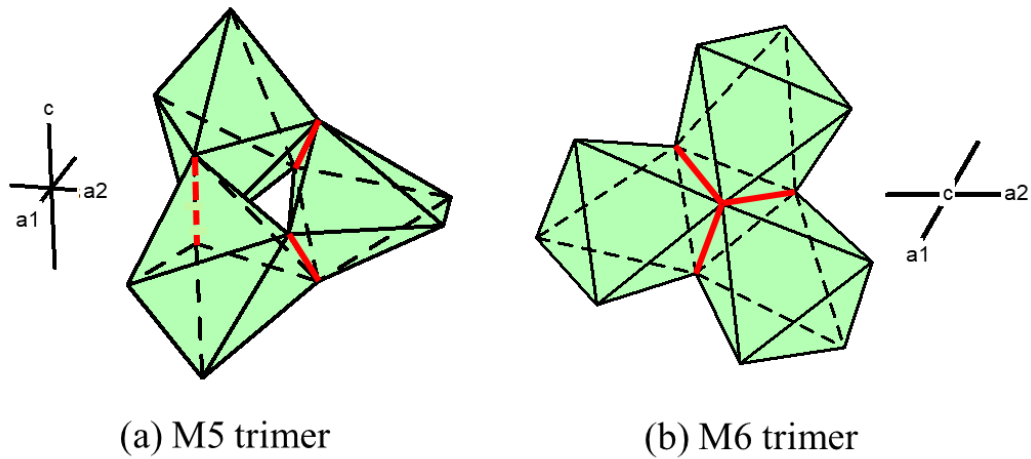
362

363

364

365

366



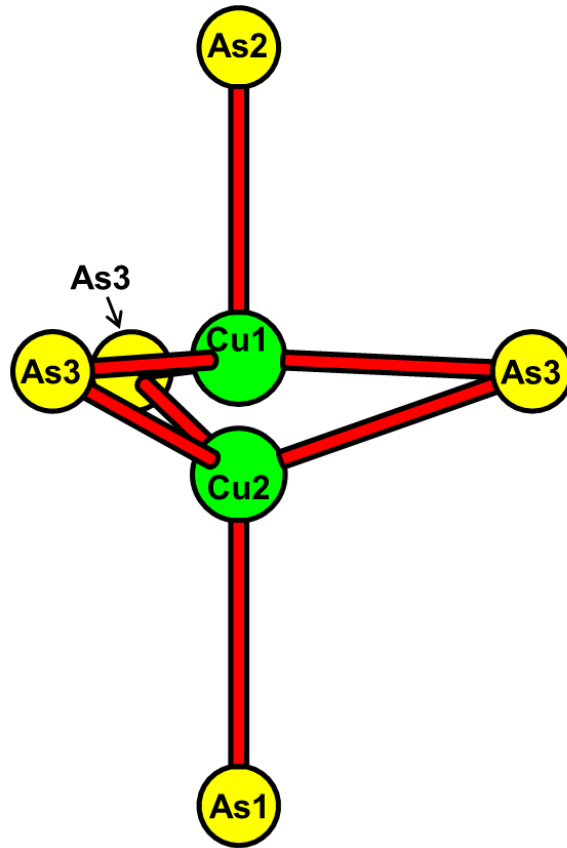
367

368

FIGURE 3. The corner-sharing M5 and edge-sharing M6 trimers in dixenite.

369

370



371

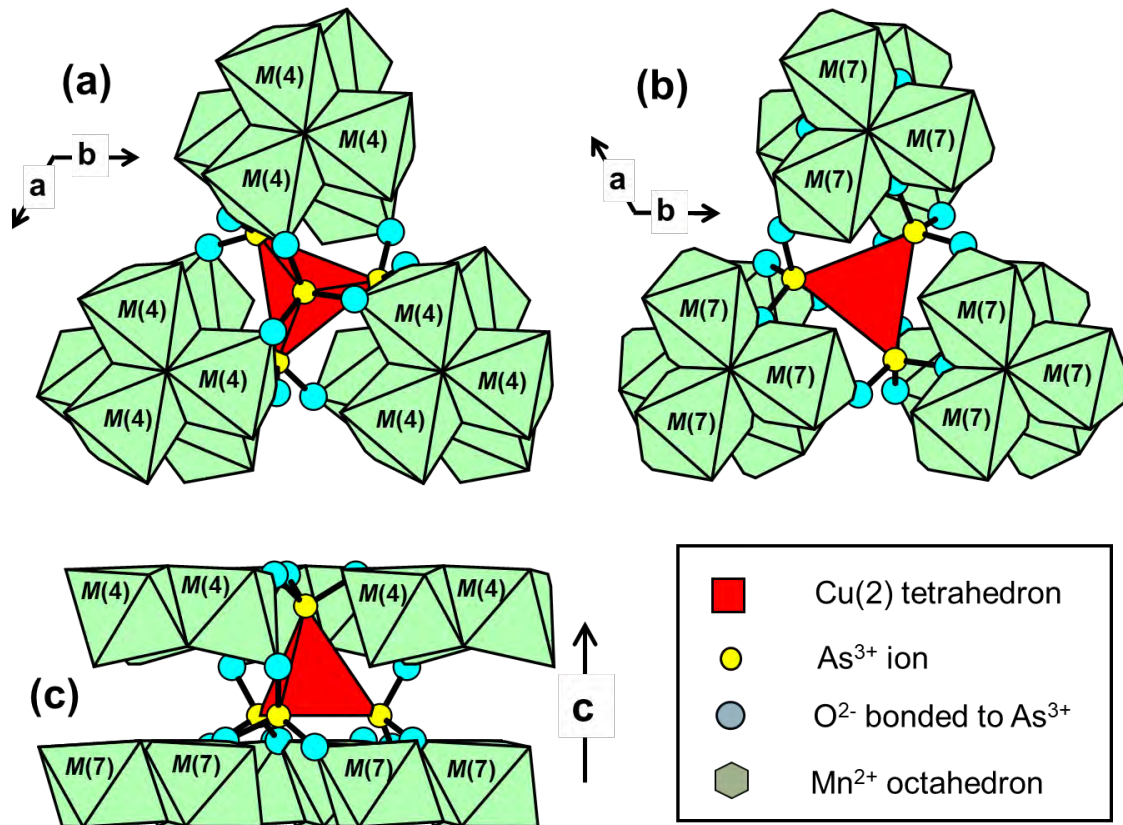
372

373

Figure 4. Coordination of split Cu1 and Cu2 sites in dixenite.

374

375



376

377

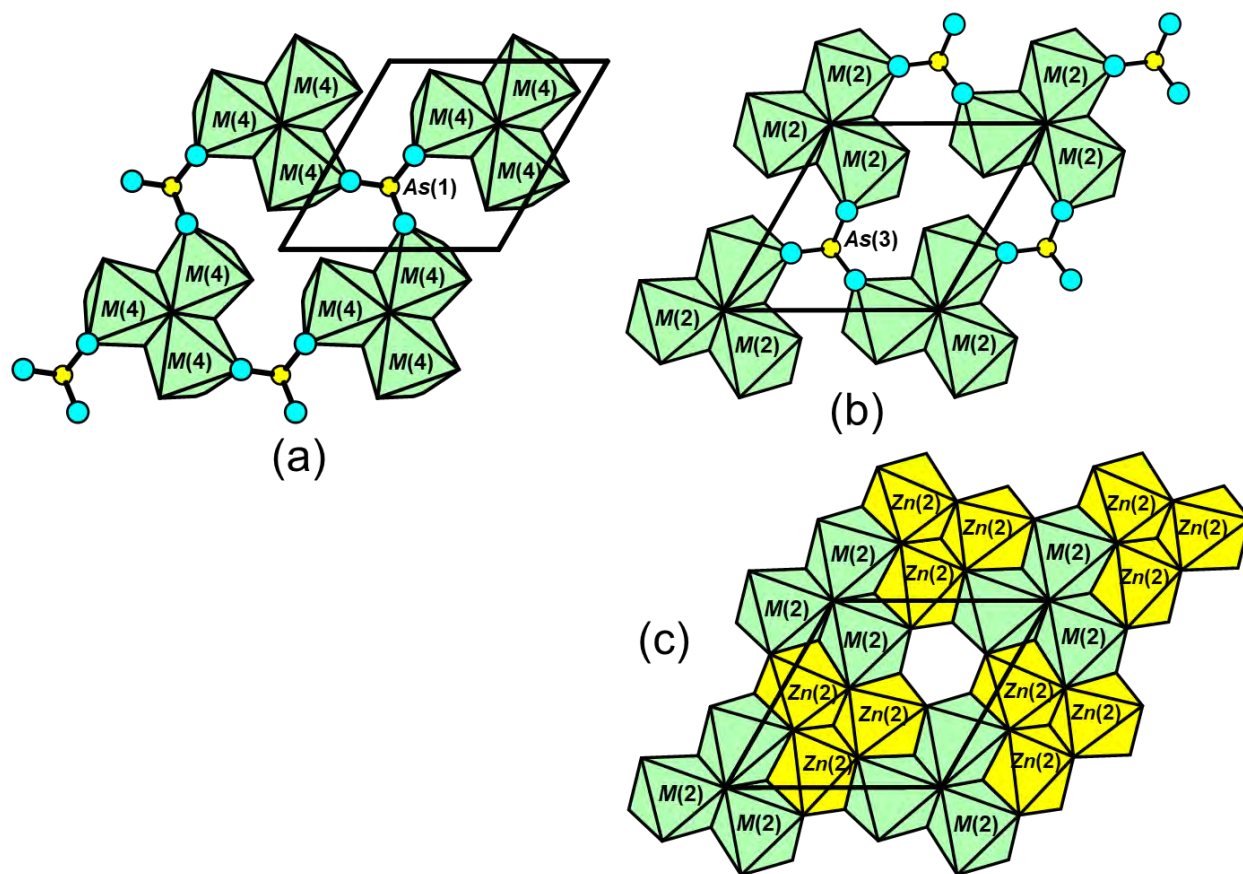
378 **FIGURE 5.** Illustration of the incorporation of $[\text{Cu}^+(\text{As}^{3+}\text{O}_3)_4]$ clusters into the layered structure.

379

380

381

382



383

384

385 Figure 6. Comparison of the M(4)-As(1) layer in dixenite with M(2)-As(3) layer in mcgovernite.

386

387

388